REPORT

⌘ *Author's Choice*

THE JOURNAL OF BIOLOGICAL CHEMISTRY VOL. 287, NO. 3, pp. 1657–1661, January 13, 2012

Beltless Translocation Domain of Botulinum Neurotoxin A Embodies a Minimum Ion-conductive Channel*

Received for publication, November 1, 2011, and in revised form, December 7, 2011
Published, JBC Papers in Press, December 12, 2011, DOI 10.1074/jbc.C111.319400

Audrey Fischer[‡1,2], **Shilpa Sambashivan**[§1,3], **Axel T. Brunger**[§¶‖], **and Mauricio Montal**[‡4]

From the [‡]*Section of Neurobiology, Division of Biological Sciences, University of California at San Diego, La Jolla, California 92093-0366, the* [§]*Department of Molecular and Cellular Physiology, Stanford University, Stanford, California 94305, the* [¶]*Departments of Neurology and Neurological Sciences, Structural Biology, and Photon Science, Stanford University, Stanford, California 94305, and the* [‖]*Howard Hughes Medical Institute, Stanford University, Stanford, California 94305*

Background: A key step in intoxication by botulinum neurotoxins is the translocation of the protease domain by the translocation domain (TD) across endosomes. The requirements for translocation remain poorly understood.
Results: A construct encompassing the TD yet devoid of the belt embodies a minimum channel-forming unit.
Conclusion: The belt is dispensable for channel formation.
Significance: The belt restricts cargo dissociation from channel during translocation.

Botulinum neurotoxin, the causative agent of the paralytic disease botulism, is an endopeptidase composed of a catalytic domain (or light chain (LC)) and a heavy chain (HC) encompassing the translocation domain (TD) and receptor-binding domain. Upon receptor-mediated endocytosis, the LC and TD are proposed to undergo conformational changes in the acidic endocytic environment resulting in the formation of an LC protein-conducting TD channel. The mechanism of channel formation and the conformational changes in the toxin upon acidification are important but less well understood aspects of botulinum neurotoxin intoxication. Here, we have identified a minimum channel-forming truncation of the TD, the "beltless" TD, that forms transmembrane channels with ion conduction properties similar to those of the full-length TD. At variance with the holotoxin and the HC, channel formation for both the TD and the beltless TD occurs independent of a transmembrane pH gradient. Furthermore, acidification in solution induces moderate secondary structure changes. The subtle nature of the conformational changes evoked by acidification on the TD suggests that, in the context of the holotoxin, larger structural rearrangements and LC unfolding occur preceding or concurrent to channel formation. This notion is consistent with the hypothesis that although each domain of the holotoxin functions individually, each domain serves as a chaperone for the others.

Botulism is a rare but serious paralytic disease caused by the obligate, spore-forming, anaerobic bacterium, *Clostridium botulinum*. The bacterium produces seven different serotypes of the botulinum neurotoxin (BoNT),[5] BoNTs A–G. All seven BoNTs are synthesized as 150-kDa single-chain polypeptides that are subsequently processed by clostridial or host cell proteases to yield the catalytically active di-chain toxins held together by a disulfide bond (1, 2). The crystal structures of BoNT/A (1), BoNT/B (3), and BoNT/E (4) reveal that the toxins are modular in design with three functionally distinct domains acting synergistically in the four-step intoxication process (2, 5, 6). The domain architecture of the BoNT/A holotoxin is illustrated in Fig. 1*A*. The 100-kDa C-terminal heavy chain (HC) is composed of an ~50-kDa translocation domain (TD or H_N) and an ~50-kDa receptor-binding domain (RBD or H_C). The RBD is composed of an N-terminal β-barrel and a C-terminal β-trefoil. The RBD determines neuronal targeting and initiates intoxication via receptor-mediated endocytosis by binding to the protein receptor SV2 for BoNT/A, BoNT/D, BoNT/E, and BoNT/F (7–9), synaptotagmin for BoNT/B (10, 11) and BoNT/G (11, 12), as well as a ganglioside co-receptor (12–14). Residence within the endosome triggers the TD, predominantly α-helical, to form a protein-conducting channel that transports the partially unfolded enzymatic moiety across the membrane of the endocytic vesicle to the cytosol (15). The 50-kDa N-terminal catalytic domain (also referred to as the light chain (LC)) is a Zn^{2+} endopeptidase that cleaves specific SNARE proteins, thereby disrupting SNARE complex assembly and subsequent neurotransmitter release (16–18). The LC has a conserved catalytic core reminiscent of thermolysin and a canonical HE*XX*H motif (19–21).

The low pH-induced conformational changes in the TD that facilitate channel formation and LC translocation are important yet less well understood aspects of BoNT intoxication (22). It has been suggested that BoNT holotoxins undergo substantial conformational changes upon acidification prior to channel formation, a model based largely on the mechanism of action of the structurally similar diphtheria and anthrax toxins (23). However, recent studies suggest that low pH does not necessar-

* This work was supported by the Howard Hughes Medical Institute. This work was also supported, in whole or in part, by National Institutes of Health Grants MH63105 (to A. T. B.), GM49711, and AI065359 (to M. M).
⌘ *Author's Choice*—Final version full access.
[1] Both authors contributed equally to this work.
[2] Present address: Johns Hopkins University Applied Physics Laboratory, Laurel, MD 20723.
[3] Supported by the Genentech Foundation postdoctoral fellowship, Stanford University. Present address: Dept. of Neurosciences, Amgen Inc., South San Francisco, CA 94080.
[4] To whom correspondence should be addressed. Tel.: 858-534-0931; Fax: 858-822-3763; E-mail: mmontal@ucsd.edu.

[5] The abbreviations used are: BoNT, botulinum neurotoxin; DDM, *n*-dodecyl β-D-maltoside; HC, heavy chain; LC, light chain; P_o, channel open probability; RBD, receptor-binding domain; TCEP, tris-(2-carboxyethyl) phosphine; TD, translocation domain; SEC-MALLS, size exclusion chromatography multi-angle laser light scattering; $V_{1/2}$, the voltage at which $P_o = 0.5$; pS, picosiemens.

ily induce large conformational changes in the TD of BoNTs (11, 24–26).

At neutral pH, the TD of BoNT/A consists of two long, highly conserved, kinked α-helices, 105 Å in length, flanked on either end by shorter helices and loops (1). It links to the LC by a belt region (see Fig. 1*A*, residues 450–491 depicted in *red* and 492–545 in *gold*), structurally reminiscent of the BoNT/A substrate SNAP-25 that saddles the LC and occludes its active site (19). This arrangement is conserved by the belts of BoNT/B (27) and BoNT/E (4). The belt has been proposed to function as an active site inhibitor as well as a low pH-induced trigger for synchronized channel formation and initiation of LC translocation (5, 28). The predicted pI of 4.66 of the N-terminal region of the TD including the belt provides support for the proposed role of this region as the acidic endosomal pH sensor (29). Experimental and computational studies on the TD have identified amphipathic regions in this N-terminal region following the belt region that could potentially participate in channel formation (30–32). Spatially proximal to one amphipathic region are Asp-612, Glu-616, Asp-588, and Glu-619, a highly conserved cluster of negative charges with a presumably higher local pK_a that render them titratable at endosomal pH (pH 5.0–5.5) (29). Interestingly, all the identified amphipathic regions and charged residues are present in loop regions or small helices distinct from the large helices of the TD, suggesting that large conformational changes may not be necessary for low pH-driven BoNT/A channel formation.

Here, we show that the belt region of BoNT/A is dispensable for channel formation given that the beltless TD forms ion-conducting channels. Although acidic pH alters the secondary structure, association with the membrane at neutral pH is sufficient to promote membrane insertion and channel formation. The protein does, however, form channels more rapidly at acidic pH when compared with neutral pH indicative of facilitated initial insertion into the membrane.

EXPERIMENTAL PROCEDURES

Expression and Purification of the Beltless TD Construct—The beltless TD (residues 546–870) was cloned into pET23a vector and expressed in *Escherichia coli* BL21 (DE3) cells. The cells were grown in LB medium to an optical density of 0.6–0.8, induced with 1 mM isopropyl-1-thio-β-D-galactopyranoside, and grown overnight at 18 °C under continuous shaking. The cells were harvested by centrifugation at 4000 rpm for 20 min, and the cell pellet was incubated for 45 min at 4 °C in a lysis buffer that contains 50 mM Tris-Cl (pH 8), 0.5 M NaCl, 1% Triton X-100, 1% Tween 20, protease inhibitor mixture (Roche Applied Science), and 1.0 mg/ml lysozyme. Subsequently, the cells were disrupted by sonication on ice for 2 min with pulsing. The cell lysate was centrifuged at 55,000 rpm for 45 min, and the supernatant was filtered before loading onto a GE Healthcare HisTrap nickel-nitrilotriacetic acid column. The protein was eluted over a 0–400 mM imidazole gradient in 0.5 M NaCl, 50 mM Tris-Cl, pH 8, 0.5% Triton X-100, and 0.5% Tween 20; the C-terminal His_6 was not removed. The eluted protein was dialyzed overnight against 50 mM Tris-Cl (pH 8), 50 mM NaCl, 0.5% Triton X-100, and 0.5% Tween 20. The next day, the protein was loaded on a MonoQ 10/10 column (GE Healthcare) equilibrated with low salt buffer, and the protein was eluted in a 0–1 M NaCl gradient buffer containing detergent. The fractions containing beltless translocation domain were pooled, concentrated, and run on a Superdex s75 16/60 preparative column (GE Healthcare) equilibrated with buffer that contains either 0.5% Triton X-100 or 0.5% *n*-dodecyl β-D-maltoside (DDM).

Size Exclusion Chromatography Multi-angle Laser Light Scattering (SEC-MALLS) Analysis—100 μl of the beltless TD at a concentration of 1 mg/ml was injected into the Shodex-803 size exclusion column pre-equilibrated with 50 mM Tris-Cl (pH 8), 150 mM NaCl, and 0.5% Triton X-100. A DAWN EOS with a K5 flow cell and a 690-nm wavelength laser were used in light scattering experiments. Refractive index measurements were performed using an OPTILAB DSP instrument with a P10 cell. A value of 0.185 ml/g was used for the d_n/d_c ratio of the protein. Monomeric bovine serum albumin dissolved in 50 mM Tris-Cl, 150 mM NaCl, and 0.5% Triton X-100 was used to normalize the detector responses. Astra software was used to analyze the SEC-MALLS data.

Circular Dichroism (CD) Spectroscopy—All CD data were collected on an AVIV 202-01 spectrometer equipped with a thermoelectric unit. Cuvettes with path lengths of 1 mm and 1 cm were used for the far-UV and near-UV measurements, respectively. Samples contained protein at 0.1 mg/ml, in the presence of 0.5% Triton X-100, 150 mM NaCl, 50 mM Tris-Cl, and CH_3COOH (to adjust pH values 4.6–5.6). Three scans were averaged for every sample, and the appropriate buffer blank was subtracted from the data. The CD data were plotted using IGOR PRO. The data were averaged for 2 s/data point and scanned at the rate of 1 nm/s. All spectra were recorded at 25 °C.

Cell Culture and Patch Clamp Recordings—Excised patches from Neuro-2A cells in the inside-out configuration were used as described (33, 34). Current recordings were obtained under voltage clamp conditions at 22 ± 2 °C. Records were acquired on an EPC-9 amplifier at a sampling frequency of 20 kHz and, where indicated, filtered online to 2 kHz using a Gaussian filter. To emulate endosomal conditions, the *trans* compartment (bath) solution contained (in mM) 200 NaCl, 5 MOPS, (pH 7.0 with HCl), 0.25 tris-(2-carboxyethyl) phosphine (TCEP), 1 $ZnCl_2$, and the *cis* compartment (pipette) solution contained (in mM) 200 NaCl, 5 MES, (pH 5.3 or pH 6.0 with HCl). When the *cis* compartment was filled with pH 7 buffer, the *trans* compartment solution set to pH 7.0 was used. The osmolarity of both solutions was determined to be ~390 mosM. $ZnCl_2$ was used to block endogenous channel activity specific to Neuro-2A cells (35, 36). BoNT reconstitution and channel insertion was achieved by supplementing 2.5 μg/ml BoNT holotoxin or beltless TD to the pipette solution, which was set to an endosomal pH of 5.3, 6.0, or 7.0.

Data Analysis of the Patch Clamp Recordings—Analysis was performed on single bursts of each experimental record using the PClamp software. Single-channel conductance (γ) was calculated from Gaussian fits to current amplitude histograms. The total number of opening events analyzed was 89,193. The voltage dependence of channel opening was calculated from measurements of the fraction of time that the channel is open (P_o) as a function of voltage by integration of γ histograms

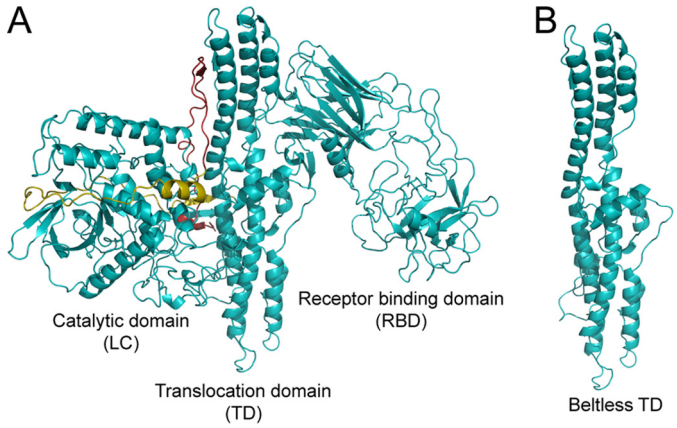

FIGURE 1. **BoNT/A domain architecture.** *A*, BoNT/A holotoxin is a tripartite structure with an N-terminal catalytic domain (LC) and a C-terminal HC composed of the TD and RBD. The LC is linked to the TD by a belt (shown in *red* and *gold*). *B*, beltless TD construct (residues 546–870). The image was rendered on YASARA (45) using the Protein Data Bank I.D. 3BTA (1).

where γ is $60 \leq \gamma \leq 75$ pS. The voltage at which $P_o = 0.5$ ($V_{½}$) was calculated from sigmoidal fits of the P_o *versus* applied voltage curves. Statistical values represent means ± S.E., unless otherwise indicated. All experiments were performed at least in triplicate.

RESULTS AND DISCUSSION

Beltless TD Undergoes Loss in Helicity at Acidic pH—To determine whether the belt is required for channel formation, we generated a TD construct devoid of the belt region beginning at residue 546 of BoNT/A (Fig. 1*B*). The beltless TD was expressed in *E. coli* and affinity-purified in the presence of Triton X-100 and Tween 20. The purity and monodispersity of the protein were confirmed by SEC-MALLS and SDS-PAGE (Fig. 2, *A* and *B*). Far-UV CD spectroscopy revealed a largely helical structure at pH 8.0 (>95% helical) with the characteristic minima at 208 nm and 222 nm at pH 8.0 (Fig. 2*C*).

To determine the effect of acidification on the secondary structure of the beltless TD *in vitro*, the protein was incubated in acetate buffer (pH range of 4.4–5.6 with increments of 0.2 pH units for 1–24 h), and the structural changes were monitored by CD spectroscopy. The deconvolution of the far-UV CD spectra of the protein revealed that acidification results in moderate loss of helical content (~30%) (Fig. 2*C*).

Beltless TD Forms Ion-conducting Channels in Neuroblastoma Neuro-2A Cells Independent of pH Gradient—Next we sought to examine the channel-forming ability of the recombinant beltless TD. The beltless TD was exchanged into DDM, a detergent compatible with channel assays. Channel formation was monitored on excised membrane patches from Neuro-2A cells under conditions that recapitulate the pH and redox gradients (Δ) across endosomes (33, 34, 37); the *cis* (endosomal) compartment containing the beltless TD was held at pH 5.3, and the *trans* (cytosol) compartment was maintained at pH 7.0 and supplemented with the membrane nonpermeable reductant TCEP. No channel activity was detected from membranes of Neuro-2A cells when supplemented with 0.5% DDM alone in the *cis* compartment (data not shown); in contrast, Na^+-conducting channels were readily observed when the beltless TD

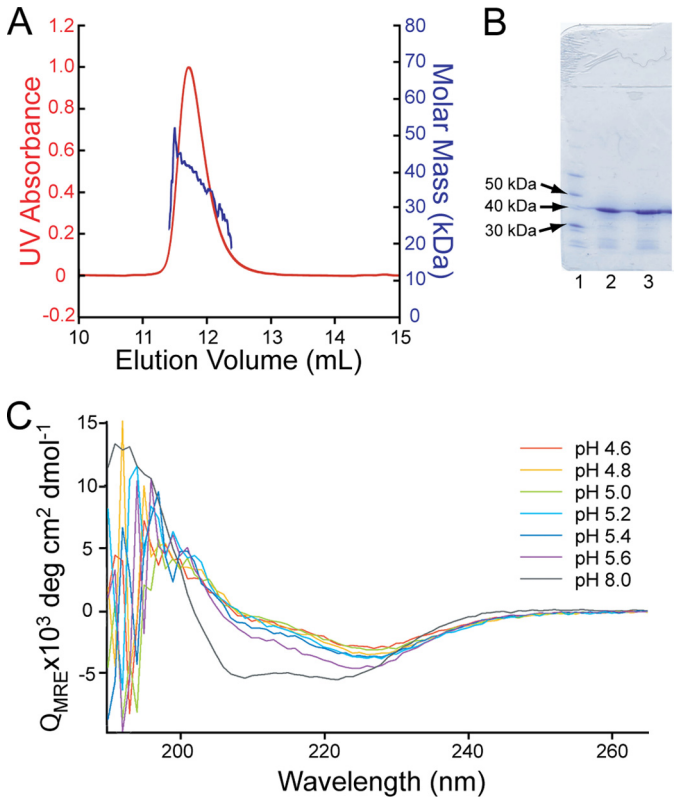

FIGURE 2. **Biochemical and structural characterization of beltless TD.** *A* and *B*, SEC-MALLS (*A*) and SDS-PAGE (*B*) analysis of the beltless TD purified from *E. coli* reveals a monomeric protein of 38 kDa. *B*, SDS-PAGE gel. *Lane 1* is a ladder marker, and *lanes 2* and *3* are aliquots of SEC-MALLS 11- and 12-ml fractions. *C*, CD analysis of the beltless TD over a range of pH values. The protein is >95% helical at pH 8.0 with the characteristic minima at 208 and 222 nm (*gray trace*). Upon acidification, it exhibits an ~30% loss in helicity. *deg*, degrees.

was added under otherwise identical conditions (Fig. 3*A*). Channel characteristics of the beltless TD were indistinguishable from those previously characterized for the intact TD and for the HC (37). Representative current records over a range of applied voltages are shown in Fig. 3*A*. Discrete channel transitions between the closed and open state are clearly discerned (Fig. 3*A*, *bottom*, *green trace*). The single-channel conductance in symmetric 200 mM NaCl was determined to be 67 ± 1 pS with the channels opening primarily at negative membrane potentials in a voltage-dependent manner (Fig. 3*A*).

To assess the effect of ΔpH (the pH gradient across the *cis* and *trans* compartments) on the channel-conducting activity of the beltless TD, three distinct experimental conditions were evaluated. The *cis* compartment was maintained at pH 5, 6, or 7, respectively, whereas the *trans* compartment was held at pH 7 supplemented with TCEP (Fig. 3*B*). The beltless TD formed channels with the same properties and similar voltage dependence irrespective of ΔpH (Fig. 3*C*). The only discernible difference between these conditions was the latency period preceding the detection of ion-conducting channels. *cis* pH 5 and pH 6 channel activity initiated on average after 14 ± 2 and 18 ± 6 min, respectively, whereas *cis* pH 7 channel activity exhibited a lag time of 29 ± 10 min of incubation.

Our findings show that the belt region of the TD is dispensable for channel formation; the beltless TD is sufficient to form

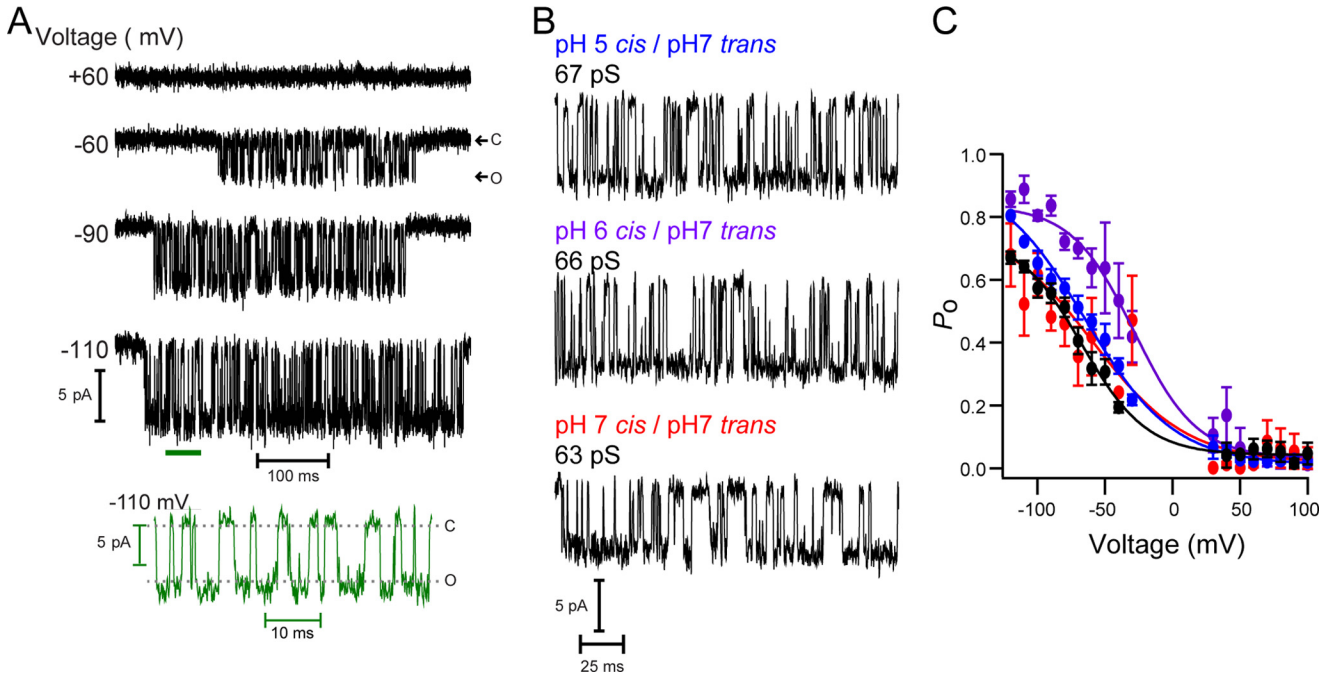

FIGURE 3. **Channel activity of beltless TD.** *A*, beltless TD channel activity was measured on excised patches of Neuro-2A cells. Representative single-channel currents were obtained at the indicated voltages; consecutive voltage pulses were applied to the same patch for each experimental condition. Channel opening is indicated by a downward deflection; *C* and *O* denote the closed and open states. γ was measured to be 67 ± 1 pS. A section of the recordings obtained at −110 mV delimited by the *green bar* is shown in the *bottom traces* at a 10-fold higher time resolution; the prototypical square events that are characteristic of unitary channel currents are clearly discerned. *B*, beltless TD channel activity is independent of ΔpH across the membrane. Representative single-channel currents are shown for each pH gradient condition measured at V = −100 mV. *C*, analysis of HC channel activity at pH 5 *cis*/pH 7 *trans* (*black*) ($V_{1/2}$ = −64.6 ± 2.2 mV), beltless TD for pH 5 *cis*/pH 7 *trans* (*blue*) ($V_{1/2}$ = −64.9 ± 2.2 mV), pH 6 *cis*/pH 7 *trans* (purple) ($V_{1/2}$ = −29.4 ± 4.2 mV), and pH 7 *cis*/pH 7 *trans* (*red*) ($V_{1/2}$ = −58.9 ± 9.0 mV).

ion-conducting channels in Neuro-2A cells. Our results indicate that although acidification induces moderate changes in secondary structure (Fig. 2*C*), channel activity occurs independent of ΔpH (Fig. 3). The rate of channel formation is accelerated at acidic pH, suggesting that for the beltless TD, acidic pH within the endosome promotes favorable kinetics of secondary structure rearrangement to a conformation competent for membrane insertion and channel formation. These features are nearly equivalent to the properties of the full-length TD (37), indicating that the belt region does not play a major role in the initial kinetics of either membrane insertion or channel formation in the absence of the LC cargo. However, productive intoxication requires an intact holotoxin, and within the holotoxin, the belt region maintains the LC in close proximity to the TD (1, 3, 4). The new results are consistent with the model (5) that the belt facilitates protein translocation by restricting dissociation of the LC cargo from the channel until the LC exits on the *trans* side and refolds within the cytosol (5, 28, 33, 34, 37). A requirement for acid-induced cargo unfolding and pore formation has been reported for the translocation of the catalytic moieties of BoNT/D (38), anthrax lethal toxin (39, 40), the *C. botulinum* C2 toxin (41, 42), and diphtheria toxin (43) through their respective translocation pores.

Although the molecular basis underlying BoNT membrane insertion and channel formation is presently unknown, we propose that it is aided by protonation of acidic residues resulting in disruption of salt bridges between amphipathic helices. The disruption of salt bridges resulting in protein destabilization has also been proposed for the ClC family of anion transporters that, like BoNT/A, also exhibit greatly reduced stability with a small effect on conformation upon acidification (44). We identified several salt bridges in the TD domains of BoNT/A, but of particular interest is a salt bridge between the side chain of Lys-592 and the Asp-612 that occurs in one of the three predicted amphipathic regions (residues 595–614) proposed to participate in channel formation. Proximal to this salt bridge is a hydrogen bond between Ser-586 and Glu-616 that would also be destabilized at low pH. Thus, it appears as if acidic pH were tuned to disrupt the interactions that hold the amphipathic helices together without evoking large conformational rearrangements, yet leading to membrane insertion. Additionally, this amphipathic region is spatially close to a loop that contains Glu-755, Glu-756, Glu-757, and Lys-758, all of which would favor interactions with a negatively charged membrane at low pH. Mutational studies designed to disrupt these interactions (Lys-592–Asp-612 and Ser-586–Glu-616, respectively) might shed further insights into the molecular mechanism by which protein destabilization and tertiary structure rearrangement result in membrane insertion, channel formation, and LC translocation.

REFERENCES

1. Lacy, D. B., Tepp, W., Cohen, A. C., DasGupta, B. R., and Stevens, R. C. (1998) Crystal structure of botulinum neurotoxin type A and implications for toxicity. *Nat. Struct. Biol.* **5,** 898–902
2. Schiavo, G., Matteoli, M., and Montecucco, C. (2000) Neurotoxins affecting neuroexocytosis. *Physiol. Rev.* **80,** 717–766
3. Swaminathan, S., and Eswaramoorthy, S. (2000) Structural analysis of the catalytic and binding sites of *Clostridium botulinum* neurotoxin B. *Nat.*

Struct. Biol. **7,** 693–699
4. Kumaran, D., Eswaramoorthy, S., Furey, W., Navaza, J., Sax, M., and Swaminathan, S. (2009) Domain organization in *Clostridium botulinum* neurotoxin type E is unique: its implication in faster translocation. *J. Mol. Biol.* **386,** 233–245
5. Montal, M. (2010) Botulinum neurotoxin: a marvel of protein design. *Annu. Rev. Biochem.* **79,** 591–617
6. Simpson, L. L. (2004) Identification of the major steps in botulinum toxin action. *Annu. Rev. Pharmacol. Toxicol.* **44,** 167–193
7. Dong, M., Yeh, F., Tepp, W. H., Dean, C., Johnson, E. A., Janz, R., and Chapman, E. R. (2006) SV2 is the protein receptor for botulinum neurotoxin A. *Science* **312,** 592–596
8. Fu, Z., Chen, C., Barbieri, J. T., Kim, J. J., and Baldwin, M. R. (2009) Glycosylated SV2 and gangliosides as dual receptors for botulinum neurotoxin serotype F. *Biochemistry* **48,** 5631–5641
9. Mahrhold, S., Rummel, A., Bigalke, H., Davletov, B., and Binz, T. (2006) The synaptic vesicle protein 2C mediates the uptake of botulinum neurotoxin A into phrenic nerves. *FEBS Lett.* **580,** 2011–2014
10. Dong, M., Richards, D. A., Goodnough, M. C., Tepp, W. H., Johnson, E. A., and Chapman, E. R. (2003) Synaptotagmins I and II mediate entry of botulinum neurotoxin B into cells. *J. Cell Biol.* **162,** 1293–1303
11. Schmitt, J., Karalewitz, A., Benefield, D. A., Mushrush, D. J., Pruitt, R. N., Spiller, B. W., Barbieri, J. T., and Lacy, D. B. (2010) Structural analysis of botulinum neurotoxin type G receptor binding. *Biochemistry* **49,** 5200–5205
12. Rummel, A., Eichner, T., Weil, T., Karnath, T., Gutcaits, A., Mahrhold, S., Sandhoff, K., Proia, R. L., Acharya, K. R., Bigalke, H., and Binz, T. (2007) Identification of the protein receptor-binding site of botulinum neurotoxins B and G proves the double-receptor concept. *Proc. Natl. Acad. Sci. U.S.A.* **104,** 359–364
13. Montecucco, C., and Schiavo, G. (1995) Structure and function of tetanus and botulinum neurotoxins. *Q Rev. Biophys.* **28,** 423–472
14. Rummel, A., Häfner, K., Mahrhold, S., Darashchonak, N., Holt, M., Jahn, R., Beermann, S., Karnath, T., Bigalke, H., and Binz, T. (2009) Botulinum neurotoxins C, E, and F bind gangliosides via a conserved binding site prior to stimulation-dependent uptake with botulinum neurotoxin F utilizing the three isoforms of SV2 as second receptor. *J. Neurochem.* **110,** 1942–1954
15. Koriazova, L. K., and Montal, M. (2003) Translocation of botulinum neurotoxin light chain protease through the heavy chain channel. *Nat. Struct. Biol.* **10,** 13–18
16. Jahn, R., and Scheller, R. H. (2006) SNAREs: engines for membrane fusion. *Nat. Rev. Mol. Cell Biol.* **7,** 631–643
17. Sutton, R. B., Fasshauer, D., Jahn, R., and Brunger, A. T. (1998) Crystal structure of a SNARE complex involved in synaptic exocytosis at 2.4 Å resolution. *Nature* **395,** 347–353
18. Weber, T., Zemelman, B. V., McNew, J. A., Westermann, B., Gmachl, M., Parlati, F., Söllner, T. H., and Rothman, J. E. (1998) SNAREpins: minimal machinery for membrane fusion. *Cell* **92,** 759–772
19. Breidenbach, M. A., and Brunger, A. T. (2004) Substrate recognition strategy for botulinum neurotoxin serotype A. *Nature* **432,** 925–929
20. Montecucco, C., and Schiavo, G. (1994) Mechanism of action of tetanus and botulinum neurotoxins. *Mol. Microbiol.* **13,** 1–8
21. Schiavo, G., Benfenati, F., Poulain, B., Rossetto, O., Polverino de Laureto, P., DasGupta, B. R., and Montecucco, C. (1992) Tetanus and botulinum-B neurotoxins block neurotransmitter release by proteolytic cleavage of synaptobrevin. *Nature* **359,** 832–835
22. Pirazzini, M., Rossetto, O., Bolognese, P., Shone, C. C., and Montecucco, C. (2011) Double anchorage to the membrane and intact interchain disulfide bond are required for the low pH-induced entry of tetanus and botulinum neurotoxins into neurons. *Cell Microbiol.* **13,** 1731–1743
23. Young, J. A., and Collier, R. J. (2007) Anthrax toxin: receptor binding, internalization, pore formation, and translocation. *Annu. Rev. Biochem.* **76,** 243–265
24. Galloux, M., Vitrac, H., Montagner, C., Raffestin, S., Popoff, M. R., Chenal, A., Forge, V., and Gillet, D. (2008) Membrane interaction of botulinum neurotoxin A translocation (T) domain: the belt region is a regulatory loop for membrane interaction. *J. Biol. Chem.* **283,** 27668–27676
25. Lai, B., Agarwal, R., Nelson, L. D., Swaminathan, S., and London, E. (2010) Low pH-induced pore formation by the T domain of botulinum toxin type A is dependent upon NaCl concentration. *J. Membr. Biol.* **236,** 191–201
26. Mushrush, D. J., Koteiche, H. A., Sammons, M. A., Link, A. J., McHaourab, H. S., and Lacy, D. B. (2011) Studies of the mechanistic details of the pH-dependent association of botulinum neurotoxin with membranes. *J. Biol. Chem.* **286,** 27011–27018
27. Agarwal, R., Schmidt, J. J., Stafford, R. G., and Swaminathan, S. (2009) Mode of VAMP substrate recognition and inhibition of *Clostridium botulinum* neurotoxin F. *Nat. Struct. Mol. Biol.* **16,** 789–794
28. Brunger, A. T., Breidenbach, M. A., Jin, R., Fischer, A., Santos, J. S., and Montal, M. (2007) Botulinum neurotoxin heavy chain belt as an intramolecular chaperone for the light chain. *PLoS Pathog.* **3,** 1191–1194
29. Lacy, D. B., and Stevens, R. C. (1999) Sequence homology and structural analysis of the clostridial neurotoxins. *J. Mol. Biol.* **291,** 1091–1104
30. Lebeda, F. J., and Olson, M. A. (1995) Structural predictions of the channel-forming region of botulinum neurotoxin heavy chain. *Toxicon* **33,** 559–567
31. Montal, M. S., Blewitt, R., Tomich, J. M., and Montal, M. (1992) Identification of an ion channel-forming motif in the primary structure of tetanus and botulinum neurotoxins. *FEBS Lett.* **313,** 12–18
32. Oblatt-Montal, M., Yamazaki, M., Nelson, R., and Montal, M. (1995) Formation of ion channels in lipid bilayers by a peptide with the predicted transmembrane sequence of botulinum neurotoxin A. *Protein Sci.* **4,** 1490–1497
33. Fischer, A., and Montal, M. (2007) Crucial role of the disulfide bridge between botulinum neurotoxin light and heavy chains in protease translocation across membranes. *J. Biol. Chem.* **282,** 29604–29611
34. Fischer, A., and Montal, M. (2007) Single-molecule detection of intermediates during botulinum neurotoxin translocation across membranes. *Proc. Natl. Acad. Sci. U.S.A.* **104,** 10447–10452
35. Carpaneto, A., Accardi, A., Pisciotta, M., and Gambale, F. (1999) Chloride channels activated by hypotonicity in N2A neuroblastoma cell line. *Exp. Brain Res.* **124,** 193–199
36. Lascola, C. D., Nelson, D. J., and Kraig, R. P. (1998) Cytoskeletal actin gates a Cl^- channel in neocortical astrocytes. *J. Neurosci.* **18,** 1679–1692
37. Fischer, A., Mushrush, D. J., Lacy, D. B., and Montal, M. (2008) Botulinum neurotoxin devoid of receptor-binding domain translocates active protease. *PLoS Pathog.* **4,** e1000245
38. Bade, S., Rummel, A., Reisinger, C., Karnath, T., Ahnert-Hilger, G., Bigalke, H., and Binz, T. (2004) Botulinum neurotoxin type D enables cytosolic delivery of enzymatically active cargo proteins to neurons via unfolded translocation intermediates. *J. Neurochem.* **91,** 1461–1472
39. Basilio, D., Juris, S. J., Collier, R. J., and Finkelstein, A. (2009) Evidence for a proton-protein symport mechanism in the anthrax toxin channel. *J. Gen. Physiol.* **133,** 307–314
40. Krantz, B. A., Finkelstein, A., and Collier, R. J. (2006) Protein translocation through the anthrax toxin transmembrane pore is driven by a proton gradient. *J. Mol. Biol.* **355,** 968–979
41. Blöcker, D., Pohlmann, K., Haug, G., Bachmeyer, C., Benz, R., Aktories, K., and Barth, H. (2003) *Clostridium botulinum* C2 toxin: low pH-induced pore formation is required for translocation of the enzyme component C2I into the cytosol of host cells. *J. Biol. Chem.* **278,** 37360–37367
42. Haug, G., Wilde, C., Leemhuis, J., Meyer, D. K., Aktories, K., and Barth, H. (2003) Cellular uptake of *Clostridium botulinum* C2 toxin: membrane translocation of a fusion toxin requires unfolding of its dihydrofolate reductase domain. *Biochemistry* **42,** 15284–15291
43. Ren, J., Kachel, K., Kim, H., Malenbaum, S. E., Collier, R. J., and London, E. (1999) Interaction of diphtheria toxin T domain with molten globule-like proteins and its implications for translocation. *Science* **284,** 955–957
44. Fanucchi, S., Adamson, R. J., and Dirr, H. W. (2008) Formation of an unfolding intermediate state of soluble chloride intracellular channel protein CLIC1 at acidic pH. *Biochemistry* **47,** 11674–11681
45. Krieger, E. (2011) *YASARA*, YASARA Biosciences, Vienna, Austria